21st Australasian Fluid Mechanics Conference
Adelaide, Australia
10-13 December 2018

Active Vibration Control of a Sphere Using Rotary Oscillations

T. McQueen, J. Zhao, J. Sheridan and M. C. Thompson

Department of Mechanical and Aerospace Engineering
Monash University, Victoria 3800, Australia

Abstract

Investigating the vortex-induced vibrations (VIV) of a sphere offers us not only the opportunity to better understand fundamentals of fluid-structure interaction, but also to develop practical control approaches of VIV. In this study, we impose high-frequency rotary oscillations on a sphere as a control method to disrupt large-scale vortex formation in the wake.

The effects of rotary oscillation frequency and amplitude were first investigated to gain an understanding of vortex suppression mechanisms and to define the bounds of open-loop control effectiveness. It was found that the effects of high-frequency rotary oscillations varied across the range of vibration modes investigated. For the mode II branch, optimal tuning of the oscillation frequency resulted in an 84% reduction in VIV amplitude. Subsequently, an attempt was made to further suppress VIV by implementing a closed-loop control system.

Introduction

Vortex-induced vibration (VIV) of cylinders and spheres occurs commonly and is often associated with detrimental structural effects. As such, the phenomenon has been extensively studied. A broad literature base details the effects of VIV on cylinders and spheres from both practical and fundamental perspectives. For both these geometries, vibration occurs due to a resonance between the fluid forces acting on the body, caused by the vortex shedding, and the natural frequency of the system. From a practical perspective, circular cylinder structures are more prevalent. Offshore oil platforms, cables, and circular towers may all experience VIV under certain operating conditions. Reviews by Williamson & Govardhan and Bearman [1, 16] reveal in detail the mechanisms contributing to VIV of cylinders. For spheres, the practical applications seem more limited, although there are still examples to be found. Krakovich et al. [7], Lee et al. [8] and Behara & Sotiropoulos [3] have revealed in their investigations of vibrating spheres that complex three-dimensional wakes initiate and sustain the oscillatory body motion. Here however, we are interested in the problem from a fundamental perspective. The sphere is a generic three-dimensional prototype and thus it offers the opportunity to investigate the fundamental effects of three-dimensionality on fluid-structure interactions.

Due to the practical importance of VIV, extensive research has been conducted to develop control methods to reduce VIV of structures. For cylinders, techniques such as fluid forcing, wake control cylinders, and body rotation have been effectively employed to suppress structural vibration [2, 4, 12, 15]. On the other hand, however, there has been much less work on VIV control of spheres. van Hout et al. [14] used acoustic control to either suppress or amplify the vibration response of a tethered sphere.

In the present paper, we examine the effect of two distinct methods of rotary oscillation on the VIV of a sphere. Firstly, high-frequency rotary oscillations, approximately one order of magnitude above the vortex shedding frequency, are implemented. The aim of this rotation setting is to disrupt the large-scale vortex formation in the wake through interaction with small-scale flow structures close to the body, in order to suppress VIV with minimal energy input. Secondly, a closed-loop proportional controller is implemented using the sphere displacement as the feedback reference signal. Sareen et al. [10] showed that the VIV response could be significantly suppressed by constant rotations imposed on a sphere. By using a closed-loop controller, the direction of rotation can be optimised over a single vibration cycle, providing potential performance benefits.

The experimental methodology is presented below. This is followed by the section of results on the open-loop control method. Finally, the conclusions are drawn. It is planned that the results for closed-loop control will be presented at the 21st Australasian Fluid Mechanics Conference.

Experimental methodology

The investigation was conducted in the free-surface water channel of the *Fluids Laboratory for Aeronautical and Industrial Research* (FLAIR) at Monash University. The water channel has a working section of 600 × 800 × 4000 mm. A 70 mm diameter sphere, which was precision-machined from Renshape 460, was mounted by a 3 mm rod to a servo motor (Maxon Motor, EC-max 4-pole 22, equipped with a rotary encoder with a resolution of 3600 counts per revolution). The servo motor was mounted to a linear air-bearing rig that constrained the sphere to move with one degree of freedom transverse to the oncoming flow. Therefore, the governing equation of motion is given by

$$m\ddot{y} + c\dot{y} + ky = F_y, \tag{1}$$

where m is the total oscillating mass, c is the structural damping factor, k is the spring constant, y is the body displacement, and F_y is the transverse fluid force (the transverse lift).

Details of the experimental setup can be found in articles by Zhao et al. [17] and Sareen et al. [10]. A schematic view of the system is shown in figure 1, which illustrates key parameters of the fluid-structure system. The top of the sphere was immersed one sphere diameter beneath the surface. The rotation axis of the sphere was perpendicular to the free surface. The servo motor was used to rotate the sphere with a sinusoidal rotation profile. Table 1 details key non-dimensional parameters used in this study. The parameters relating to the rotary oscillations are discussed below.

Equation 2 defines the rotation profile of the sphere and introduces the two parameters used to vary the rotary oscillations, namely: rotation amplitude (Ω_0) (peak angular velocity); and forcing rotation frequency (f_r). These two parameters are normalised as per Equations 3 and 4, and referred to as the rotation ratio and forcing frequency ratio respectively.

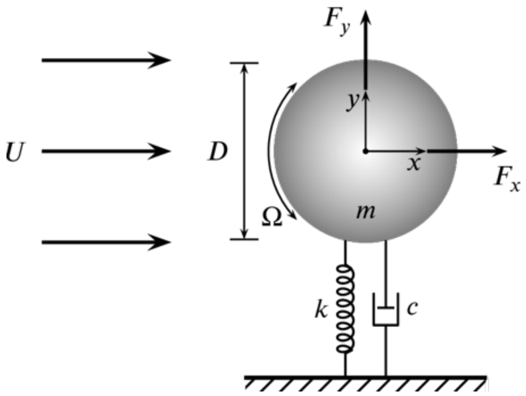

Figure 1: Schematic of the experimental set-up. The sphere is constrained to one degree of freedom transverse to the free-stream flow. D is the sphere diameter; U is the free-stream velocity; c is the structural damping factor; k is the spring constant; m is the total oscillating mass; Ω_0 is the angular velocity; F_x and F_y are the streamwise (drag) and the transverse (lift) force components acting on the body, respectively.

Amplitude Ratio	A^*	$\frac{A}{D}$
Damping Ratio	ζ	$\frac{c}{2\sqrt{k(m+m_a)}}$
Reduced Velocity	U^*	$\frac{U}{f_{nw}D}$
Mass Ratio	m^*	$\frac{m}{m_d}$

Table 1: Non-dimensional parameters. A is the structural vibration amplitude; D is sphere diameter; m is the total oscillating mass; m_a is the added mass, defined by $m_a = C_A m_d$, where C_A is the added-mass coefficient (0.5 for a sphere); c is the structural damping factor; k is the spring constant; U is the free-stream velocity; f_{nw} is the natural frequency of the system in quiescent water; m_d is the mass of the displaced fluid.

$$\Omega = \Omega_0 \sin(2\pi f_r t) \quad (2)$$

$$\alpha_r{}^* = \frac{D\Omega_0}{2U} \quad (3)$$

$$f_r{}^* = \frac{f_r}{f_{nw}} \quad (4)$$

Sphere oscillations were measured using a linear encoder (RGH24, Renishaw, UK) with resolution of 1 μm at a sampling rate of 100 Hz. Each dataset consisted of at least 80 vibration cycles.

The mass ratio of the system, defined as the ratio of the mass of the system (m) to the displaced mass of the fluid (m_d), was $m^* = m/m_d = 10.1$. The structural damping and natural frequency of the system in quiescent water were measured to be $\zeta = 4.22 \times 10^{-3}$ and $f_{nw} = 0.267$ Hz respectively. The free-stream velocity was varied from 0.14 ms^{-1} to 0.30 ms^{-1}, corresponding to a Reynolds number range of $4 \times 10^3 \leq Re = UD/\nu \leq 2.2 \times 10^4$, with ν denoting the kinematic viscosity of the fluid. The reduced velocity range was $3 \leq U^* \leq 17$. The rotation ratio was set to $\alpha_r{}^* = 0.1$ for the investigation. The forcing frequency ratio was varied from $5 \leq f_r^* \leq 35$. The upper limit was due to torque limitations of the servo motor. Table 1 details the non-dimensional parameters used in this investigation.

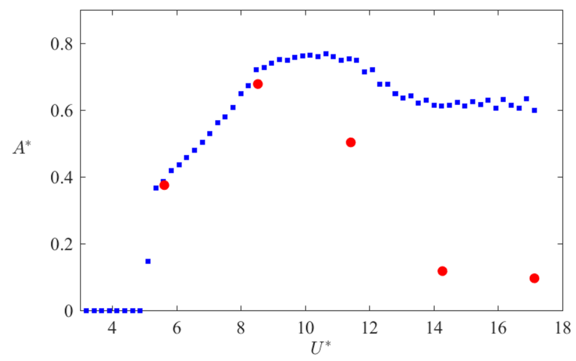

Figure 2: Amplitude response of the sphere for no rotation (blue squares) and with imposed rotary oscillations (red circles). The results for rotary oscillations show the maximum reduction in amplitude response of the sphere across the range of imposed forcing frequency ratios.

To implement the closed-loop proportional controller, Beckhoff Automation hardware and corresponding software, TwinCat 3, was used in conjunction with a desktop computer. The system consisted of a coupler (EK1100, Beckhoff Automation) to connect the the hardware with the desktop computer, a digital input (EL1124, Beckhoff Automation) to record sphere displacement, and a Maxon motor controller (MAXPOS 50/5, Maxon Motors) to control sphere rotation. The real-time sampling rate of the system was 4kHz. The proportional controller consisted of a single gain block that controlled sphere rotation in proportion to the normalised sphere displacement.

Results

The experimental setup was first validated by comparing results obtained without rotary oscillations to those of Govardan & Williamson [5] and Sareen et al. [10]. Overall, as shown in figure 2, good agreement was found with the instigation of vibrations and the subsequent trend of the response.

Rotary oscillations were then implemented at a range of reduced velocities across the mode I, mode II, and transition to mode III regimes. At each reduced velocity the frequency of the oscillations was varied from $5 < f_r{}^* < 35$. In the mode I regime, the amplitude response of the sphere was insensitive to the rotary oscillations. This observation is consistent with the results of Sareen et al. [10, 11], who found that it was more difficult for constant and low-frequency rotary oscillations to affect the amplitude response in the mode I regime, where the vortex shedding frequency was close to the natural frequency of the system.

Beyond the peak of the mode II regime, the rotary oscillations have an appreciable effect on the amplitude response. At $U^* = 11.5$, a reduction up to 34% is observed in the amplitude response. After the peak of mode II, the rotary oscillations also have a noticeable effect on the phase between the transverse lift and the body displacement. At $U^* = 11.5$, for the lowest forcing frequency ratios examined, there is an increase of approximately 25° in total phase. As the forcing frequency ratio is increased, the total phase decreases to a minimum of 20° below that of the non-rotary case.

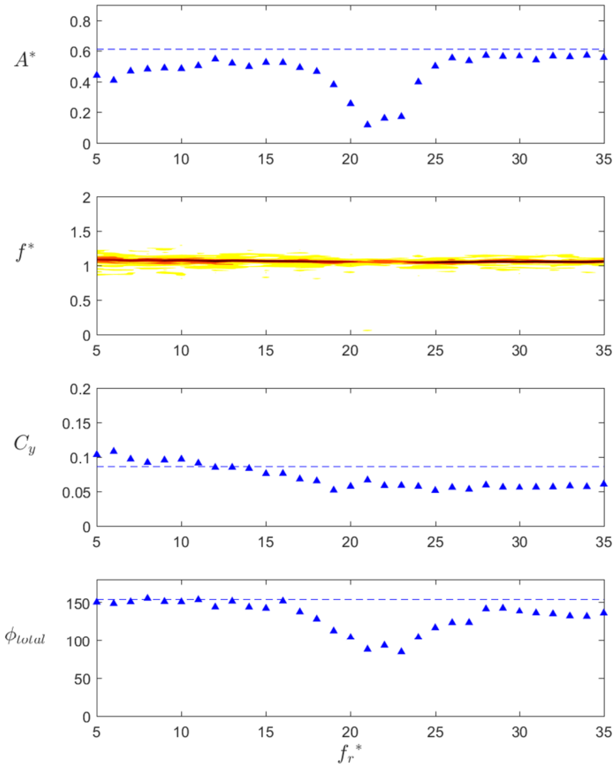

Figure 3: The response of the sphere with imposed rotary oscillations as a function of f_r with $\alpha_r{}^* = 0.1$ at $U^* = 14$. From top to bottom, the figures show: the amplitude response; the power spectra of body vibrations; the transverse lift force; and total phase (phase between the body vibrations and fluid force). The dotted line shows the result for no rotary oscillations.

As seen in figure 3, at $U^* = 14$, there is a significant attenuation of the amplitude response (up to 81%) for a relatively narrow band of forcing frequency ratios. There is a decrease in total phase around $f_r{}^* = 22$, from 150° to 90°, corresponding directly to the attenuation of the vibration response. From the frequency power spectra of the sphere displacement, it can be seen that there is no obvious change in the body vibration frequency across the $f_r{}^*$ range investigated.

At the highest reduced velocity investigated, $U^* = 17$, there is a step decrease in the total phase corresponding to a step change in the amplitude response (84% reduction) at $f_r{}^* = 20$ (figure 4). In conjunction with the phase variation observed at $U^* = 14$ and $U^* = 11.5$, this observation suggests that, if we were to implement a closed-loop control system, attempting to manipulate the phase difference between the fluid force and the body displacement would be more efficient than attempting to directly reduce the magnitude of the fluid force itself.

For $U^* = 17$, large scatter in the data can be observed for very high forcing frequencies. Examining the time series of the vibration response for this reduced velocity at select forcing frequency ratios reveals a potential cause of this. Figure 5 shows sample time series of the sphere displacement at $f_r{}^* = 31$. The vibration response is rapidly attenuated around a non-dimensionalised time of 40 and remains minimal for a period of approximately 15 vibration cycles. This phenomenon appears to happen sporadically with no distinct peak in the fre-

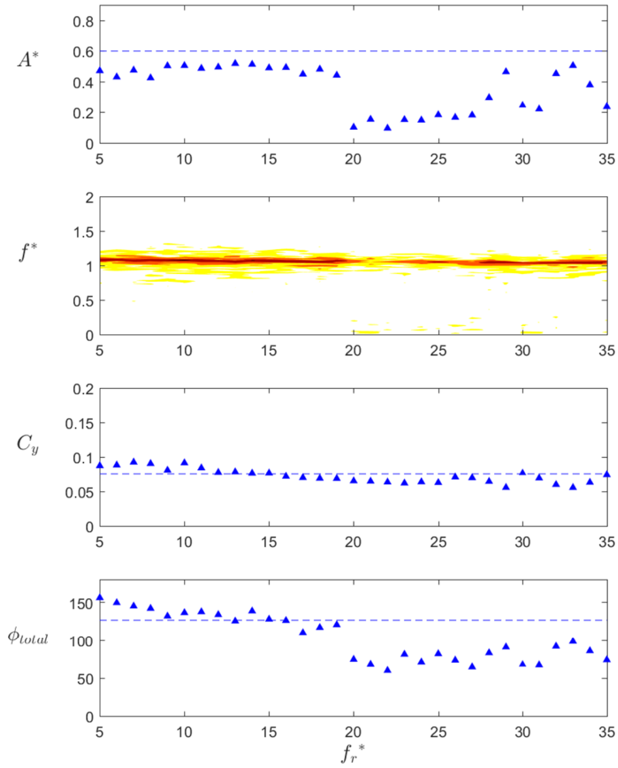

Figure 4: The response of the sphere with imposed rotary oscillations as a function of f_r with $\alpha_r{}^* = 0.1$ at $U^* = 17$. Refer to figure 3 for further details.

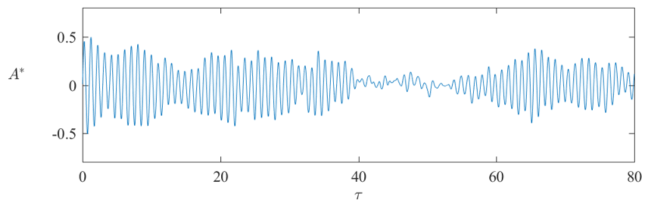

Figure 5: Time series of sphere displacement at $U^* = 17$, $f_r^* = 31$, $\alpha_r^* = 0.1$. Time has been non-dimensionalised by the sphere oscillation period.

quency spectra for these low-frequency pulsations. This suggests that wake is characterised by two states: the first state where the effect of the rotary oscillations dominates the system and minimal vibrations occur; and the second state where the rotary oscillations have minimal effect on the vortex shedding process results in large vibrations.

Phase-averaged PIV data was acquired in the equatorial plane of the sphere for select reduced velocities and forcing frequency ratios. Where the vibrations were suppressed, there were no observable major differences in the phase-averaged wake structure. This observation is inline with that of Tokumaru & Dimotakis [13], who found that the effect of high-frequency rotary oscillations imposed on a fixed cylinder was primarily only observable in the shear layers separating from the body.

Sakamoto & Haniu [9] conducted their experiments and collated past results for flow over a fixed sphere. They described the existence of a low-mode Strouhal number associated with wave-like motion of the wake, and a high-mode Strouhal number associated with the small-scale instability of the separating shear layer. Where a noticeable attenuation of the vibration response was observed in this investigation, at $U^* = 14$ and $U^* = 17$, the frequency of rotary oscillations were approximately 6 - 12 times the low-mode, and 45% to 75% of the high-mode, Strouhal numbers of the equivalent fixed body. It is hypothesised that the rotary oscillations are interacting with the separating shear layer in a manner that affects the periodicity, timing, and perhaps to a lesser degree the strength of the vortex shedding.

Conclusions

This initial investigation shows promise for suppression of VIV of a sphere through sinusoidal rotation at low amplitude and frequencies approaching that of the shear layer instability. It was found that, with careful frequency selection, it was possible to substantially suppress VIV in the mode II and transition to mode III regimes. Where VIV was significantly suppressed, the vibrations became less periodic and a reduction in the total phase was observed. No major variations to the phase-averaged wake structure were observed in the equatorial plane of the sphere. It will be of interest in our further investigation to utilise time-resolved PIV to reveal the effect of rotary oscillations on the flow dynamics and to analyse the results of the proportional controller.

Acknowledgements

The authors would like to acknowledge the financial support of the Australian Research Council through grants DP150102879 and DP170100275. TM acknowledges the financial support of an Australian Government Research Training Program Scholarship.

References

[1] Bearman, P.W., *Annu. Rev. Fluid Mech.*, 1984, 195–222.

[2] Chen, W., Xin, D., Xu, F., Li, H., Ou, J., Hu, H, Suppression of vortex-induced vibration of a circular cylinder using suction-based flow control, *J. Fluids and Structures*, 2013, 42:25–39

[3] Behara, S., Sotiropoulos, F., Vortex-induced vibrations of an elastically mounted sphere: The effects of Reynolds number and reduced Velocity, *J. Fluids and Structures*, 2016, 54–68.

[4] Du, L., Sun, X., Suppression of vortex-induced vibration using the rotary oscillations of a cylinder, *Physics of Fluids*, 2015, 27:023603

[5] Govardhan, R.N., Williamson, C.H.K., Vortex-induced vibrations of a sphere, *J. Fluid Mech.*, 2005, 531:11–47.

[6] Jauvtis, N., Govardhan, R., Williamson, C.H.K., Multiple modes of vortex-induced vibration of a sphere, *Journal of Fluids and Structures*, 2001, 555–63.

[7] Krakovich, A., Eshbal, L., van Hout, R., Vortex dynamics and associated fluid forcing in the near wake of a light and heavy tethered sphere in uniform flow, *Exp. Fluids*, 2013, 54:1615.

[8] Lee, H., Hourigan, K., Thompson, M.C., Vortex-induced vibration of a neutrally buoyant tethered sphere, *J. Fluid Mech.*, 2013, 719:97–128.

[9] Sakamoto, H., Haniu, H., A study on vortex shedding from spheres in a uniform flow, *J. Fluids Engineering*, 1990, 112:386–92

[10] Sareen, A., Zhao, J., Lo Jacono, D., Sheridan, J., Hourigan, K., Thompson, M.C., Vortex-induced vibration of a rotating sphere, *J. Fluid Mech.*, 2018,

[11] Sareen, A., Zhao, J., Sheridan, J., Hourigan, K., Thompson, M.C., The effect of imposed rotary oscillation on the flow-induced vibration of a sphere, *J. Fluid Mech.*, (Submitted),

[12] Silva-Ortega, M., Assi, G.R.S., Suppression of the vortex-induced vibration of a circular cylinder surrounded by eight rotating wake-control cylinders, *J. Fluids and Structures*, 2017, 74:401–12

[13] Tokumaru, P.T., Dimotakis, P.E., Rotary oscillation control of a cylinder wake, *J. Fluid Mech.*, 1991, 224:77–90

[14] van Hout, R., Katz, A., Greenblatt, D., Acoustic control of vortex-induced vibrations of a tethered sphere, *AIAA Journal*, 2013, Vol.51, No.3.

[15] Vicente-Ludlam, D., Barrero-Gill, A., Velazquez, Flow-induced vibration control of a circular cylinder using rotational oscillation feedback, *J. Fluid Mech.*, 2018, 847:93–118.

[16] Williamson, C.H.K., Govardhan, R., Vortex-induced vibrations, *Annu. Rev. Fluid Mech.*, 2004, 413–55.

[17] Zhao, J., Leontini, S.J., Lo Jacono, D., Sheridan, J., Fluid-structure interaction of a square cylinder at different angles of attack, *J. Fluid Mech.*, 2014, 747:688–721.